"This document is the unedited Author's version of a Submitted Work that was subsequently accepted for publication in Nano Letters, copyright © American Chemical Society after peer review. To access the final edited and published work see http://pubs.acs.org/doi/abs/10.1021/nl904141r."

NANO LETTERS

pubs.acs.org/NanoLett

A Path to Ultranarrow Patterns Using Self-Assembled Lithography

Yeon Sik Jung,[†,§] J. B. Chang,[†] Eric Verploegen,[†] Karl K. Berggren,[‡] and C. A. Ross*[,†]

[†]Department of Materials Science and Engineering and [‡]Department of Electrical Engineering and Computer Science, Massachusetts Institute of Technology, 77 Massachusetts Avenue, Cambridge, Massachusetts 02139

ABSTRACT The templated self-assembly of block copolymer (BCP) thin films can generate regular arrays of 10−50 nm scale features with good positional and orientational accuracy, but the ordering, registration and pattern transfer of sub-10-nm feature sizes is not well established. Here, we report solvent-annealing and templating methods that enable the formation of highly ordered grating patterns with a line width of 8 nm and period 17 nm from a self-assembled poly(styrene-*b*-dimethylsiloxane) (PS-PDMS) diblock copolymer. The BCP patterns can be registered hierarchically on a larger-period BCP pattern, which can potentially diversify the available pattern geometries and enables precise pattern registration at small feature sizes. Sub-10-nm-wide tungsten nanowires with excellent order and uniformity were fabricated from the self-assembled patterns using a reactive ion etching process.

KEYWORDS Block copolymer, poly(dimethylsiloxane), solvent anneal, nanowire, self-assembly

Block copolymer (BCP) nanolithography has attracted much attention due to its high resolution, cost effectiveness, scalability, and compatibility with well-established planar processing techniques.[1−11] It relies on the thermodynamically driven microphase separation of block copolymers consisting of two (or more) immiscible blocks, forming periodic nanoscale structures such as arrays of spheres, cylinders, or lamellae.[12,13] The self-assembly of BCP films can be guided by chemical or topographic template patterns fabricated with conventional lithography tools to form a variety of patterns relevant to devices, such as arrays of parallel lines or close-packed posts.[2−5,7,9,14−16]

The compatibility of BCP self-assembly with conventional lithography processes and its high throughput have made it an important option for nanofabrication needs beyond the resolution limits of optical lithography. The utility of BCP patterning can be further enhanced by increasing the long-range order and minimizing defect formation during BCP microphase separation, by extending the range of available pattern dimensions into the sub-10-nm regime, by developing reliable pattern-registration processes, and by demonstrating convenient pattern transfer into functional materials. In this Letter, we address these four critical challenges by demonstrating exceptionally long-range ordered high-resolution patterns with an 8 nm line width, a double-patterning process based on the self-registration between two BCP patterns, and fabrication of well-ordered 9-nm-wide W nanowires.

For a BCP, the ordering quality, defect levels, and scalability to smaller period are all improved by selecting a material with a high Flory−Huggins interaction parameter χ, which quantifies the driving force for microphase segregation. In particular, the ultimate line-edge roughness achievable in BCP patterns is expected to be limited by the width of the intermaterial dividing surface between the microdomains (which scales with $\chi^{-0.5}$),[17] rather than by the radius of gyration of the polymer molecules. In this study, we choose PS-PDMS (Figure 1a) for its high χ parameter. Two cylinder-forming PS-PDMS BCPs were used for the self-assembled pattern-generation process. The substrates consisted of Si with native oxide that were coated with a hydroxyl-terminated PDMS homopolymer to form a 3−4 nm thick PDMS brush layer.[16,18−20] Prior to brush coating, some of the substrates were patterned with 40-nm-deep periodic trench patterns using a Lloyd's mirror interference lithography system with a He−Cd laser (wavelength = 325 nm). BCP films were spin-coated and treated with various solvent vapors for 3−25 h at room temperature to facilitate self-assembly of a monolayer of PDMS cylinders oriented parallel to the substrate. Reactive ion etching of the BCP film in CF_4 then oxygen produced parallel lines of oxidized PDMS, and this pattern was transferred into a W film using dry etching processes. Details of these experimental techniques are given in the Methods section below.

We first discuss the formation of well-ordered linear patterns from a cylindrical-morphology BCP with molecular weight (M_w) of 45.5 kg/mol. Our prior work[16,20,21] has shown that thin films of this BCP form an array of parallel cylinders with period ∼34 nm upon annealing in a saturated vapor of toluene at room temperature. By optimizing the substrate preparation and solvent annealing conditions, we were able to lower the defect levels in the array considerably. Panels b and c of Figure 1 show scanning electron microcopy (SEM)

* Corresponding author: e-mail, caross@mit.edu; tel, 617-258-0223; fax, 617-252-1020.

[§] Present address: Department of Materials Science and Engineering, Korea Advanced Institute of Science and Technology, 373-1 Guseong-dong, Yuseong-gu, Daejeon 305-701, Republic of Korea.

Received for review: 12/15/2009
Published on Web: 02/10/2010

© 2010 American Chemical Society

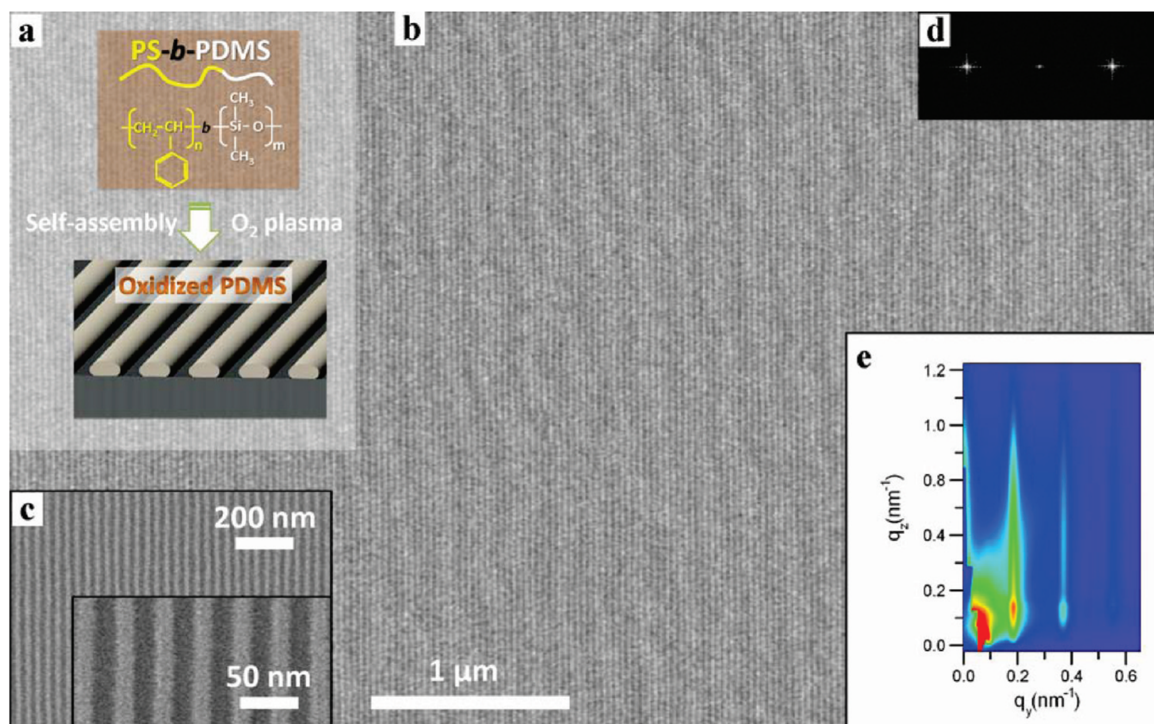

FIGURE 1. (a) A sketch of the structure of PS-PDMS block copolymer and schematic view of the oxidized PDMS cylinders after oxygen etching. (b) SEM image of an oxidized PDMS line pattern from a cylinder-forming PS-PDMS block copolymer (M_w = 45.5 kg/mol) showing excellent long-range ordering. The image size is 5.5 μm × 3.6 μm, and the BCP film was guided by 10-μm-wide trench patterns (not visible). (c) Magnified images of smaller areas of the array. (d) A fast Fourier transform of the low-magnification image. (e) The GISAXS pattern of the oxidized PDMS line pattern collected from a cm^2 area.

images of an etched BCP film on a substrate patterned with 10 μm wide trenches. The PDMS cylinders are aligned along the trench walls, and the pattern is free of defects over at least a 6-μm-diameter area, as confirmed by Figure 1b. The measured average period, line width and line edge roughness are 33.8 ± 0.41, 14.2 ± 0.2, and 3.2 ± 0.5 nm, respectively. The good ordering and low defect level are attributed to the high Flory−Huggins interaction parameter ($\chi \sim 0.26$ at room temperature[22]), which leads to a large interfacial energy between the blocks and a high-energy penalty for forming defects. Fast Fourier transform (FFT) results are shown in Figure 1d and in Figure S6a in the Supporting Information. The FFT image is characterized by two sharp spots away from the center, corresponding to high-frequency linear features with a regular periodicity. Grazing-incidence small-angle X-ray scattering (GISAXS) analysis in Figure 1e shows sharp diffraction patterns including well-resolved high-order peaks and confirms the formation of a uniform monolayer of cylinders over the incident beam area (ca. cm^2 scale) with periodicity 33.4 ± 0.86 nm.

Despite the excellent order achieved in these 14 nm line width, 34 nm period features, reducing the line width below ~10 nm while maintaining the pattern quality is not straightforward. The segregation strength (χN) decreases with the reduction of the number of repeating units, N, in the polymer chain, requiring a high-χ BCP and appropriate annealing to ensure that microphase segregation will occur. BCP patterns with sub-10-nm features have recently been reported,[11,23] but their lithography applications are restricted by poor etch selectivity between the blocks or by limited ordering. To investigate the self-assembly of a lower-N block copolymer, we examined ordering in a second PS-PDMS BCP with M_w = 16 kg/mol, annealed under a range of different solvent vapors. Results are shown in Figure 2 and in Figure S3 and Figure S4 in Supporting Information. The ordering quality was assessed (Figure 2k) by calculating the ratio of average contour length to average end-to-end distance of the cylinders (a measure of straightness) and the density of cylinder terminations or Y-junction defects. Fourier transforms of the images were also calculated (Figure S6b in Supporting Information).

In this BCP, the solvent had a dramatic effect on the quality of ordering, with acetone producing the best results. Moreover, the vapor pressure of the solvent is also important, with higher quality ordering resulting from the use of a slowly drying vapor (i.e., a vapor pressure that decreased gradually to zero) instead of a saturated vapor. The slowly drying acetone vapor produced arrays of parallel cylinders with 17.5 nm period and 8 nm line width. The cylinders demonstrate excellent long-ranger order on a flat substrate (Figure S4 in Supporting Information) and parallel alignment within linear trench walls (Figure 3a). The line edge roughness was 1.04 ± 0.27 nm, smaller than that (2.26 ± 0.92 nm) of the same BCP annealed in saturated acetone vapor.

© 2010 American Chemical Society

DOI: 10.1021/nl904141r | Nano Lett. 2010, 10, 1000--1005

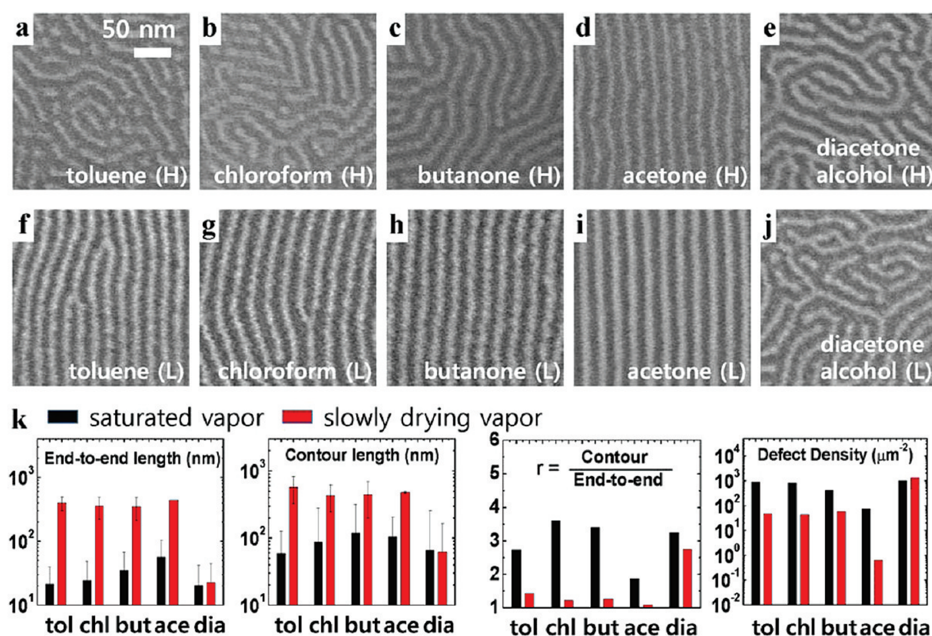

FIGURE 2. (a−k) SEM images of the oxidized PDMS patterns from a small molecular-weight PS-PDMS (M_w = 16 kg/mol) treated with saturated vapors (a−e) or slowly drying vapors (f−j). (a) and (f), toluene, (b) and (g), chloroform, (c) and (h), butanone, (d) and (i), acetone, and (e) and (j), diacetone alcohol. H and L indicate samples from saturated (high pressure) vapor and slowly drying (low pressure) vapors, respectively. A marked improvement in ordering was observed for the slowly drying vapors compared to the cases of saturated vapors. (k) Image analysis results. The end-to-end and contour lengths indicate the point-to-point distance and the fully stretched distance between the two ends of the cylinders in each image. For the better-ordered samples shown in (f−i), the estimated cylinder lengths were limited by the image size. The ratio (r) between the two lengths is a measure of straightness, and $r = 1$ for a completely straight line. The defect density measures the number of cylinder terminations and Y-junctions per unit area.

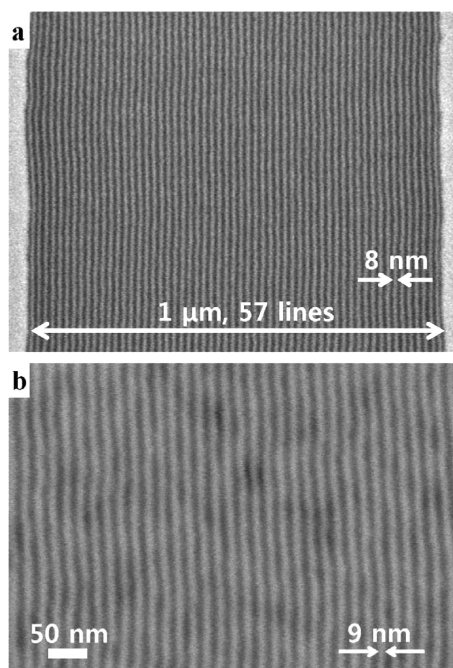

FIGURE 3. (a) Self-assembled patterns annealed in slowly drying acetone vapor on a 1-μm-wide topographic trench pattern, showing excellent order. (b) Well-aligned W nanowires with 9 nm line width prepared using the 16 kg/mol PS-PDMS.

The height of the lines, estimated from cross-sectional SEM, was 6−7 nm.

This result differs qualitatively from the behavior of 45.5 kg/mol PS-PDMS, which orders best in toluene or chloroform vapors, and not particularly well in acetone (Figure S1 in Supporting Information). During solvent-annealing, the effective χ decreases linearly with solvent volume fraction in the film[24] because of the screening effect of the solvent molecules at the interfaces between the blocks. This reduces the thermodynamic driving force for microphase segregation. Thus, there is a trade-off between enhanced diffusivity and lowered driving force, both of which result from solvent uptake by the film. This suggests that there is an optimum solvent vapor pressure to obtain good ordering. In the PS-PDMS used here, we expect the degree of swelling, and therefore the diffusivity, to be highest for toluene or chloroform vapors because the solubility parameter of the majority block, PS ($\delta = 18.5$), is well matched with those of toluene ($\delta = 18.3$) or chloroform ($\delta = 18.7$).[25,26] However, for the 16 kg/mol PS-PDMS we believe that the decrease in χ caused by these solvents limits the microphase segregation. A high segregation strength (χN) can be maintained by instead using a vapor from a less good solvent such as acetone vapor ($\delta = 19.7$), which does not lower χ as much. Moreover, annealing in slowly drying solvent vapors (evaporation rate ∼0.13−1.08 μL cm^{-2} min^{-1}, Figure 2f−j) improves the ordering compared to annealing in a saturated vapor followed by quenching. We believe that, as the vapor pressure slowly decreases, the morphology that formed at the opti-

© 2010 American Chemical Society

DOI: 10.1021/nl904141r | Nano Lett. 2010, 10, 1000–-1005

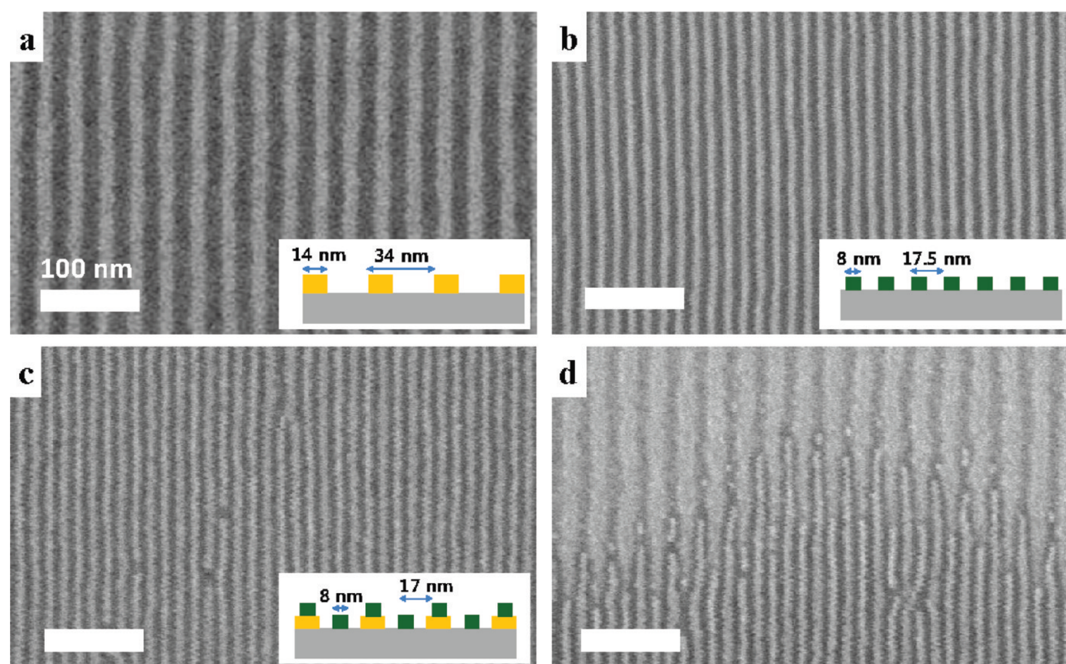

FIGURE 4. Illustration of the double patterning process. The 34-nm-period BCP patterns guide the self-assembly of a 17-nm-period BCP. (a, b) Monolayer of cylinders of 45.4 kg/mol (34-nm-period/14-nm-line width) and 16 kg/mol (17.5-nm-period/8-nm-line width) PS-PDMS respectively. (c, d) Demonstration of double patterning. The 34-nm-period BCP patterns were self-assembled in 1.3-μm-wide trench patterns, coated with a PDMS brush, followed by the self-assembly of 8-nm-wide BCP line patterns.

mum vapor pressure is kinetically trapped as the solvent concentration decreases. Use of a lower vapor pressure was ineffective in improving ordering of the 45.5 kg/mol BCP (Figure S2 in Supporting Information), which has a lower diffusivity (the diffusivity scales[27] with $\exp[-\chi N]$). These general considerations for solvent annealing are expected to apply to other BCP systems and suggest general strategies for selecting the processing conditions for small molecular weight block copolymers.

We also demonstrate fabrication of nanowires by transferring the linear patterns from PS-PDMS BCPs into more robust materials such as metals. A W film was deposited onto the oxidized-PDMS patterns and etched back to form a reverse-contrast image of the PDMS pattern.[19] Figure 3b shows a well-aligned array of W nanowires after the pattern-transfer process. The good ordering of the BCP patterns was preserved without the formation of defects such as line breaks or terminations.

We now describe a method to accurately register sub-10-nm BCP patterns on the substrate. Prior work has shown that the locations of BCP microdomains in two dimensions can be registered by chemical[4,8,9,15] or topographical[7] features of similar size to the microdomains. These template features are typically made using electron-beam lithography. However, for sizes below 10 nm, the accurate fabrication of sub-10-nm template structures becomes challenging. The alternative registration method proposed here consists of a double-patterning process in which one BCP serves as the template for another BCP of smaller period (Figure 4). Although one BCP has previously been used to template another of similar period,[28] there has been no demonstration of subdivision of the period of a larger-period BCP by a smaller.

In this hierarchical process, the microdomains of the larger-period BCP are first registered to relatively large substrate features made by conventional lithography, and in turn these microdomains template the microdomains of the smaller-period BCP. Parallel lines of oxidized PDMS with a pitch of 34 nm and height of ~12 nm (Figure 4a) were fabricated from the 45.5 kg/mol PS-PDMS BCP on a substrate with trenches, then a layer of 16 kg/mol BCP was self-assembled on top (Figure 4c,d). The 17 nm period lines were templated by the underlying 34 nm period pattern. The registration between the two different BCP patterns is evident from Figure 4d in which the overlying 16 kg/mol film was partly removed. The 8 nm wide lines in the 16 kg/mol overlayer form both between and above the lines in the underlying 45.5 kg/mol layer. Compared to a single-layer of lines formed from the 16 kg/mol BCP (Figure 4b), the double-patterned structure has alternating line widths (8 and 12 nm) and the spacing between the lines is reduced to 7 nm.

This double-patterning process bears some analogies to double-exposure photolithography,[29] proposed for the 32 and 22 nm half-pitch semiconductor manufacturing nodes, in which two separate exposures on a single photoresist layer are shifted by a half-pitch distance in order to obtain subdiffraction resolution. Unlike optical double-exposure, however, the BCP double-patterning process can lead to a diverse range of morphologies by selecting the two BCPs appropriately. For example, in addition to the patterns with

© 2010 American Chemical Society

DOI: 10.1021/nl904141r | *Nano Lett.* **2010,** *10,* 1000--1005

alternating line widths shown here, morphologies such as close-packed concentric ring arrays[21] might be formed by templating a small-period cylindrical BCP on an array of close-packed spheres, or within the close-packed holes of a perforated lamella of a larger-period BCP pattern, or square arrays may be formed using a square-symmetry triblock terpolymer[30] as template. Figure S5 (Supporting Information) shows an example in which a spherical-morphology BCP was templated on an underlying grating pattern, where the close-packed directions of the sphere array self-assembled parallel to the grating. This process has the potential to produce a variety of small-period BCP patterns without the need to directly fabricate small-period templates and can also produce structures with a more complex three-dimensional height profile compared to that from a single layer BCP.

In summary, we have demonstrated the formation of PS-PDMS BCP linear patterns with period of 17 nm, line width of 8 nm and extremely good long-range ordering by a solvent annealing process using a low vapor pressure of a moderately good solvent. These patterns can be registered on a substrate by self-aligned double patterning using a BCP with twice the period. The 17 nm period patterns were transferred into a tungsten film to make nanowire arrays with line width of 9 nm. These processes are expected to be applicable to a range of high-χ BCPs. The compatibility of these ordering, registration, and pattern transfer processes with existing planar processing technology will enable the fabrication of highly integrated nanoscale devices based on self-assembly.

Methods. ***Template Fabrication.*** The substrates for BCP self-assembly were lithographically patterned Si wafers with native oxide. The 40 nm deep periodic trench patterns were generated by using a Lloyd's Mirror interference lithography system with a He−Cd laser (λ = 325 nm). Linear grating patterns with a periodicity of 1.3 μm and above were defined in a positive resist (PFI-88, Sumitomo Chemical Co. Ltd.). A reactive ion etch (RIE) with CF_4 plasma was used to transfer the grating into the Si substrates, resulting in 40-nm-deep trench patterns. A PDMS brush was grafted on the topographic template patterns by spin-casting a hydroxyl-terminated PDMS homopolymer (M_n = 5 kg/mol, Polymer Source) and annealing the polymer film at 130 °C for 5 h to facilitate the dehydration reaction between the functionalized homopolymer and the silica surface. The role of the PDMS brush is to improve the correlation length and uniformity of the self-assembled pattern by enhancing the diffusivity of the BCP film, as reported previously.[16] The thickness of the grafted brush layer was estimated to be around 3−4 nm by optical ellipsometry.

Block Copolymer Self-Assembly. Diblock copolymers of PS-PDMS with overall molecular weights of 45.5 and 16 kg/mol and volume fraction of PDMS, f_{DMS} = 33.5% and 32.9%, respectively, were purchased from Polymer Source, Inc. To obtain uniform thin films with thicknesses of 35 nm (for M_w = 45.5 kg/mol) and 20 nm (for M_w = 16 kg/mol), toluene solutions of 1.5% (for M_w = 45.5 kg/mol) and 1% (for M_w = 16 kg/mol) by weight of the block copolymer were spin-coated on the patterned substrates. To facilitate microphase separation, the BCP films were treated with various solvent vapors such as chloroform, toluene, butanone, acetone, and diacetone alcohol in a chamber with a controlled leak at room temperature. With a constant evaporation rate, the slowly drying vapor has a partial pressure scaling with ~(time)$^{-1}$, so that the block copolymer films are exposed to a gradually decreasing vapor pressure until complete drying after 3−25 h, depending on the solvent. During the anneal, the block copolymer flowed into the trenches of the substrate, leaving the mesas free of cylinders.

Pattern-Transfer by Reactive Ion Etching. The annealed BCP films were first treated with a 5 s, 50 W, CF_4 plasma and then a 22 s, 90 W, O_2 plasma to remove first the PDMS surface layer and then the PS matrix to leave oxygen-plasma-modified PDMS cylinders on the substrate.[16] The plasma treatment time was shorter for the smaller molecular weight BCP. A W thin film with a thickness of 55 nm was deposited using an rf sputtering system (base pressure = 1×10^{-8} Torr, working pressure = 2 mTorr, and power = 300 W) on top of the block copolymer patterns and etched with a 450 W, 10 mTorr CF_4 plasma for 2 min. Initially the metallic film was relatively slowly sputter-etched by ionized CF_x species, but after the buried block copolymer patterns were exposed to the plasma, they were removed much faster than the metallic films by forming volatile SiF_x.[19] As a result, W nanowires were obtained with reverse contrast compared to the oxidized PDMS patterns.

Characterization. The surface morphologies of self-assembled BCP and metallic nanowires were observed using a Zeiss/Leo Gemini 982 scanning electron microscope operated at 5 kV. The samples were coated with a thin Au−Pd alloy film in order to reduce charging effects. Grazing-incidence small-angle X-ray scattering (GISAXS) experiments were performed at the G1 beamline at the Cornell High Energy Synchrotron Source (CHESS). The wavelength of the incident beam was 1.239 Å, with a sample to detector distance of 1122 mm and an incidence angle of 0.1°. A slow-scan CCD-based X-ray detector was used for data collection.

Acknowledgment. We gratefully acknowledge financial support from the Semiconductor Research Corporation and the Office of Naval Research.

Supporting Information Available. Additional information showing effects of solvent vapor on the ordering, double patterning from two BCPs, and fast Fourier transform analysis patterns. This material is available free of charge via the Internet at http://pubs.acs.org.

REFERENCES AND NOTES

(1) Park, M.; Harrison, C.; Chaikin, P. M.; Register, R. A.; Adamson, D. H. *Science* **1997**, *276*, 1401–1404.

© 2010 American Chemical Society

DOI: 10.1021/nl904141r | *Nano Lett.* **2010,** *10,* 1000–-1005

(2) Segalman, R. A.; Yokoyama, H.; Kramer, E. J. *Adv. Mater.* **2001**, *13*, 1152–1155.
(3) Cheng, J. Y.; Ross, C. A.; Thomas, E. L.; Smith, H. I.; Vancso, G. J. *Adv. Mater.* **2003**, *15*, 1599–1602.
(4) Kim, S. O.; Solak, H. H.; Stoykovich, M. P.; Ferrier, N. J.; de Pablo, J. J.; Nealey, P. F. *Nature* **2003**, *424*, 411–414.
(5) Black, C. T.; Bezencenet, O. *IEEE Trans. Nanotechnol.* **2004**, *3*, 412–415.
(6) Cheng, J. Y.; Mayes, A. M.; Ross, C. A. *Nat. Mater.* **2004**, *3*, 823–828.
(7) Bita, I.; Yang, J. K. W.; Jung, Y. S.; Ross, C. A.; Thomas, E. L.; Berggren, K. K. *Science* **2008**, *321*, 939–943.
(8) Cheng, J. Y.; Rettner, C. T.; Sanders, D. P.; Kim, H. C.; Hinsberg, W. D. *Adv. Mater.* **2008**, *20*, 3155–3158.
(9) Ruiz, R.; Kang, H. M.; Detcheverry, F. A.; Dobisz, E.; Kercher, D. S.; Albrecht, T. R.; de Pablo, J. J.; Nealey, P. F. *Science* **2008**, *321*, 936–939.
(10) Tang, C. B.; Lennon, E. M.; Fredrickson, G. H.; Kramer, E. J.; Hawker, C. J. *Science* **2008**, *322*, 429–432.
(11) Park, S.; Lee, D. H.; Xu, J.; Kim, B.; Hong, S. W.; Jeong, U.; Xu, T.; Russell, T. P. *Science* **2009**, *323*, 1030–1033.
(12) Leibler, L. *Macromolecules* **1980**, *13*, 1602–1617.
(13) Bates, F. S.; Fredrickson, G. H. *Annu. Rev. Phys. Chem.* **1990**, *41*, 525–557.
(14) Segalman, R. A.; Hexemer, A.; Kramer, E. J. *Phys. Rev. Lett.* **2003**, *91*, 196101.
(15) Stoykovich, M. P.; Muller, M.; Kim, S. O.; Solak, H. H.; Edwards, E. W.; de Pablo, J. J.; Nealey, P. F. *Science* **2005**, *308*, 1442–1446.
(16) Jung, Y. S.; Ross, C. A. *Nano Lett.* **2007**, *7*, 2046–2050.
(17) Broseta, D.; Fredrickson, G. H.; Helfand, E.; Leibler, L. *Macromolecules* **1990**, *23*, 132–139.
(18) Bita, I.; Yang, J. K. W.; Jung, Y. S.; Ross, C. A.; Thomas, E. L.; Berggren, K. K. *Science* **2008**, *321*, 939–943.
(19) Jung, Y. S.; Jung, W.; Ross, C. A. *Nano Lett.* **2008**, *8*, 2975–2981.
(20) Jung, Y. S.; Jung, W.; Tuller, H. L.; Ross, C. A. *Nano Lett.* **2008**, *8*, 3776–3780.
(21) Jung, Y. S.; Jung, W.; Ross, C. A. *Nano Lett.* **2008**, *8*, 2975–2981.
(22) Nose, T. *Polymer* **1995**, *36*, 2243–2248.
(23) Park, S. M.; Park, O. H.; Cheng, J. Y.; Rettner, C. T.; Kim, H. C. *Nanotechnology* **2008**, *19*, 455304.
(24) Helfand, E.; Tagami, Y. *J. Chem. Phys.* **1972**, *56*, 3592–3601.
(25) Barton, A. F. M. *CRC handbook of solubility parameters and other cohesion parameters*; CRC Press: Boca Raton, FL, 1983.
(26) Barton, A. F. M. *CRC handbook of polymer-liquid interaction parameters and solubility parameters*; CRC Press: Boca Raton, FL, 1990.
(27) Lodge, T. P.; Dalvi, M. C. *Phys. Rev. Lett.* **1995**, *75*, 657–660.
(28) Ruiz, R.; Sandstrom, R. L.; Black, C. T. *Adv. Mater.* **2007**, *19*, 587–591.
(29) Finders, J.; Dusa, M.; Vleeming, B.; Hepp, B.; Maenhoudt, M.; Cheng, S.; Vandeweyer, T. In Double patterning lithography for 32 nm: critical dimensions uniformity and overlay control considerations. *Symposium on Advanced Lithography, San Jose, CA, Feb 24—29, 2008*; SPIE—Society of Photoptical Instrumentation Engineers: Bellingham, WA, 2008.
(30) Chuang, V. P.; Gwyther, J.; Mickiewicz, R. A.; Manners, I.; Ross, C. A. *Nano Lett.* **2009**, *9*, 4364–4369.

© 2010 American Chemical Society

DOI: 10.1021/nl904141r | *Nano Lett.* **2010,** *10,* 1000--1005